01 Jan 1992

Hybrid Clamping in NTSC Digital Video Equipment

Norman R. Cox
Missouri University of Science and Technology, nrc@mst.edu

Douglas William Irwin

Recommended Citation

N. R. Cox and D. W. Irwin, "Hybrid Clamping in NTSC Digital Video Equipment," *IEEE Transactions on Broadcasting*, Institute of Electrical and Electronics Engineers (IEEE), Jan 1992.
The definitive version is available at https://doi.org/10.1109/11.127422

HYBRID CLAMPING IN NTSC DIGITAL VIDEO EQUIPMENT†

Douglas W. Irwin
McDonnel-Douglas Missile Systems, Co
P.O. Box 516
St..Louis, Mo 63166

Norman R. Cox
Dept. of Electrical Engineering.
University of Missouri-Rolla
Rolla, Mo 65401

ABSTRACT

This paper describes two algorithms that are suitable for deriving the blanking level of a National Television Systems Committee (NTSC) composite video signal. One method consists of averaging digitized color-burst samples taken from successive scan lines. A second method involves processing a group of samples taken from a single burst interval. Either algorithm used in a hybrid clamping arrangement results in automatic drift compensation and the ability to tie the back porch or sync tip to a predetermined digital output code. This aids in matching the analog signal to the input of the analog-to-digital (A/D) converter for maximum signal-to-noise ratio (SNR). In analyzing the effect of additive noise and timing jitter, it was found that both algorithms are, generally, more vulnerable than a conventional keyed clamper. However, these clampers should still perform quite well in a broadcast environment where the SNR is usually high and a stable sampling clock is readily available. Variations of these algorithms are applicable to digital coder-decoder (codec) interfaces and NTSC-compatible monitors with digital processing.

I. INTRODUCTION

Clamping circuits are used extensively throughout video transmission systems to perform dc and low-frequency restoration. These circuits also perform the important tasks of reducing low-frequency interference (hum) and minimizing "bounce" due to signal switching. A similar circuit is needed whenever an analog video signal is converted into a digital pulse-code modulation (PCM) signal. The clamper, in this case, establishes a corresponding reference between the analog and digital domains and is instrumental in matching the analog signal to the input range of the A/D converter.

A conventional analog clamper, such as the "keyed" clamper, is sometimes used ahead of the A/D converter, as shown in Fig. 1. The main disadvantage of this arrangement is that the system is susceptible to small direct current (dc) errors due to the drifting of component values in the analog and A/D converter circuits. This problem can be avoided with a digital implementation. The method illustrated in Fig. 2, for example, first computes the difference between the digitized value and the desired value of the sync tip or back porch. This value is then stored and added to each sample of the video line. Unfortunately, a sizeable portion of the A/D converter's dynamic range must be reserved for the expected signal excursions caused by changes in average picture level. The result is a lower SNR than that theoretically possible with the given A/D converter.

The hybrid clamper, shown in Fig. 3, avoids both of these problems by using digitized samples to compute the correction voltage for the analog clamper. The feedback voltage needed for dc restoration is, essentially, computed over an extended period of time, while the analog clamper is available to respond quickly on a line-by-line basis for hum removal. This method of clamping has four advantages:

1) it automatically compensates for any errors caused by drifting component values in the analog or A/D converter circuitry,
2) in conjunction with automatic gain control, it provides optimal matching of the signal amplitude to the expected input range of the A/D converter, thereby maximizing the SNR,
3) it allows back porch clamping without distorting the color burst, (if needed for system transparency), and
4) it has the ability to stabilize the blanking level, sync tip, or other datum to a predetermined digital output code.

This last advantage is particularly useful in that it allows digital deletion and reinsertion of the blanking interval.

While hybrid clamping can be a straightforward process when the signal is in monochrome or

†A major portion of this work was performed by Mr. D. W. Irwin as a partial requirement for the M.S.E.E. degree from the University of Missouri-Rolla.

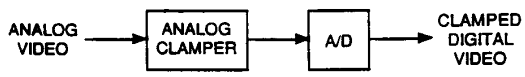

Fig. 1 Conventional Analog Clamping.

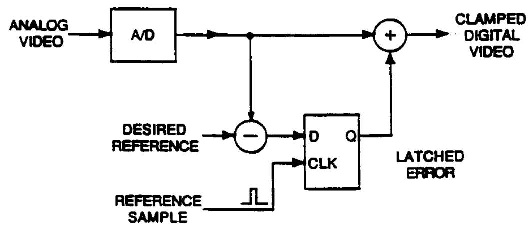

Fig. 2 A Method of Digital Clamping.

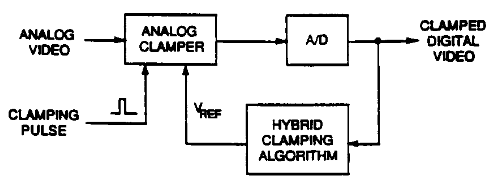

Fig. 3 Hybrid Clamping.

component format [1], back porch clamping of a composite signal is complicated by the presence of the color subcarrier reference burst. Using a single digitized sample from each back porch results in a "piano key" effect [2] due to the alternating phase of the subcarrier on adjacent scan lines. Suitable processing is required to minimize this effect and to provide adequate noise immunity.

In this paper, we describe two simple algorithms that are suitable for deriving the blanking level value from a subset of the color-burst samples. Variations of these two algorithms can be used with, virtually, any sampling rate or sampling pattern of interest. Both algorithms have been implemented in the laboratory and analyzed for their sensitivity to clock jitter and random noise. These algorithms were developed for use in a high-speed digital video simulator [3], but the basic concept is directly applicable to digital video transmission equipment, processors, codecs, and NTSC-compatible digital monitors.

II. ALGORITHMS FOR HYBRID CLAMPING

A. Averaging Samples from Adjacent Lines

One way to eliminate the piano-key effect is to simply average two color burst samples taken from two successive scan lines. Since the subcarrier component of each sample is identical in amplitude, but opposite in phase, the subcarrier components cancel each other when the two samples are averaged. The result is the average of two samples of the blanking level. Referring to Fig. 4, the dc value of the blanking level at point (i,j) can be estimated as

$$\hat{D}(i,j) = \frac{X(i,j) + X(i-1,j)}{2} \tag{1}$$

where $\hat{D}(i,j)$ is the calculated estimate of the blanking level D(i,j), and X(i,j) is the jth sample of the ith (present) line. This estimate is exact under ideal noise-free conditions, because the chrominance component C(i,j) is equal to -C(i-1,j). To improve noise immunity, a running average of an even number of samples can be computed. One possible implementation is shown in Fig. 5. In this case, the estimate of D(i,j) is

$$\hat{D}(i,j) = \frac{1}{K}\sum_{k=0}^{K-1} X(i-k,j) \tag{2}$$

where K is the even number of samples being averaged.

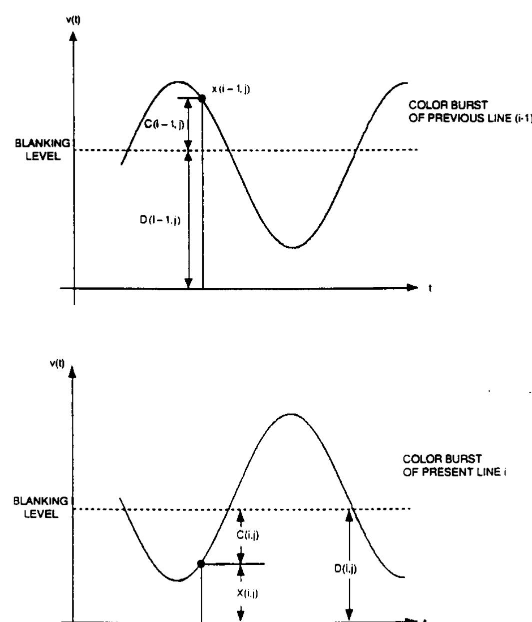

Fig. 4 Subcarrier cancellation by averaging samples from adjacent lines.

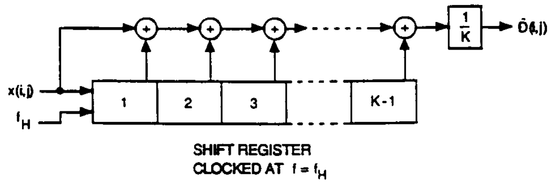

Fig. 5 One possible arrangement for averaging a larger number of samples to obtain better noise immunity.

This algorithm is always valid when the samples are vertically aligned. Considering that the video signal must be sampled at a rate greater than $2 \times 4.2\text{MHz} = 8.4$ Megasamples/s, the available sampling rates for aligned samples are

$$f_s = mf_h \quad m = 534,\ 535,\ 536,\ \ldots$$

where f_h = the horizontal scanning rate. This technique can often be applied even when samples are not vertically aligned (for example, when $f_s = 3f_{sc}$). However, care must be taken in selecting the particular samples to be averaged so that the correct subcarrier component pairs are obtained for cancellation.

B. Averaging Multiple Samples in Each Line

A second algorithm for calculating the dc level of the back porch involves averaging a small group of samples taken from the center of each color burst interval. Referring to Fig. 6, the dc value in the vicinity of point (i,j) of the back porch can be estimated as

$$\hat{D}(i,j) = \frac{1}{N}\sum_{n=0}^{N-1} X(i, j-n) \qquad (3)$$

This equation will be recognized as the computation of the first discrete Fourier transform (DFT) component of an N-point sequence. This calculation will result in the correct dc value as long as the sample values are periodic with N.

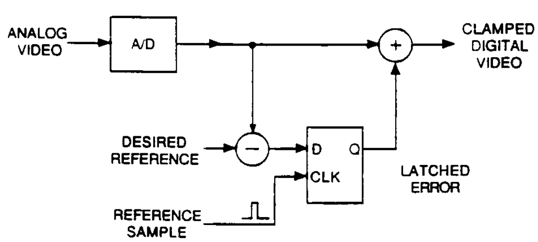

Fig. 6 Samples used for computing the dc component of the color-burst interval.

As an example, consider the case where $f_s = \frac{8}{3}f_{sc} = 9.55$ Megasamples/s. Assuming that the color burst amplitude remains constant, sample values will repeat every eight samples, hence $N = 8$. Since the sampling interval is $T_s = 1/f_{sc} = 3/8f_{sc}$, a sequence of eight samples corresponds to exactly three complete subcarrier cycles.

Vertically aligned samples are not required for this algorithm, although the length of the sequence N is limited by the length of the color burst. As a practical matter, the N samples must be taken from the center of the burst interval where the subcarrier component is fairly constant in amplitude. It is also desirable for N to be a power of two so that division can be simplified. If an aligned sampling pattern is used, this algorithm can be combined with the one-sample-per-line algorithm previously described. The number of samples may then be arbitrarily large, and samples may be taken at any point within the burst interval. For example, if eight samples are taken during each burst interval and a running average is taken over four line times, the estimate of the dc level becomes

$$\hat{D}(i,j) = \frac{1}{N \cdot K}\sum_{k=0}^{K-1}\sum_{n=0}^{N-1} X(i-k, j-n)$$

$$= \frac{1}{32}\sum_{k=0}^{3}\sum_{n=0}^{7} X(i-k, j-n) \qquad (4)$$

Even if the sample values are not periodic with N, the subcarrier component of each sample is cancelled by the corresponding subcarrier of the previous line.

III. ALGORITHM SENSITIVITY TO NOISE AND CLOCK JITTER

Although signal noise affects the accuracy of the hybrid clamper, this is less of a factor than is timing jitter. Errors due to random noise are attenuated due to the fact that a number of samples are averaged to obtain the clamping feedback voltage. In addition, digital clipping and long-term integration can be used to further dampen the system and prevent erratic behavior. The time constant of the keyed clamper can also be optimized to minimize the effect of high-frequency interference [4]. The effects of timing jitter, however, are not so easily dispelled.

A. Effect of Timing Jitter on the One-Sample-per-Line-Method

For an ideal composite video signal, we can express the color burst interval as

$$V(t) = D + A\sin\left(2\pi f_{sc} t + \phi_{sc}\right) \tag{5}$$

where V(t) is the video signal in volts or IRE units*, D is the dc level of the back porch, A is the peak value of the subcarrier reference burst, and ϕ_{SC} is the relative phase of the subcarrier. The portion of the color burst that is most sensitive to timing jitter is the region about the point of maximum slope or where

$$A\sin\left(2\pi f_{sc} t + \phi_{sc}\right) = 0 \tag{6}$$

This is illustrated in Fig. 7 for a timing offset of Δt. The peak clamping error $E_p(\Delta t)$ can be predicted as

$$E_p(\Delta t) = D - \frac{V(t_1) + V(t_2)}{2} = -\frac{\left\{A\sin\left[2\pi f_{sc}\left(\frac{-\Delta t}{2}\right)\right]\right.}{2} - \frac{\left.A\sin\left[2\pi f_{sc}\left(\frac{+\Delta t}{2}\right) + \pi\right]\right\}}{2} \tag{7}$$

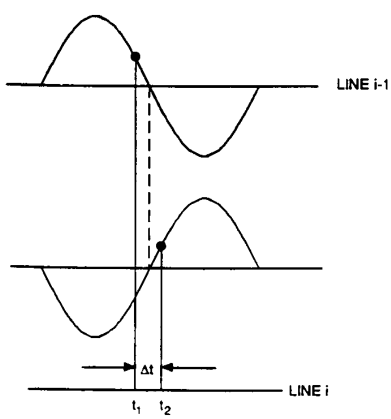

Fig. 7 Sensitivity to timing jitter is greatest about the point of maximum color-burst slope.

An equally important expression relates the dc clamping error to the frequency jitter. Frequencies that cause small amounts of constant error in the dc level are not detectable by the human eye. On the other hand, frequencies that cause the error to change in a quasi-periodic manner produce interference patterns that are quite noticeable. If we assume, for the purpose of illustration, that a single sinusoidal jitter component is present, it can be shown (see Appendix A) that the calculated dc error from line to line at any time t is

$$E(t) = -\frac{A\sin\left\{2\pi f_{sc}\left[t - \frac{1}{f_h} + B\sin\left(2\pi f_j / f_h + \phi_j\right)\right] + \phi_{sc}\right\}}{2} - \frac{A\sin\left[2\pi f_{sc}\left(t + B\sin\phi_j\right) + \phi_{sc}\right]}{2} \tag{8}$$

where f_j is the jitter frequency, B is the peak deviation of the sampling jitter in seconds, and f_j is the relative phase of the sinusoidal clock jitter. It can be seen in (8) that if the jitter frequency is an integer multiple of f_h(i.e., $f_j = mf_h$, for $m = 1, 2, 3, \ldots$), E(t) goes to zero, since $f_h = 2f_{sc} / 455$. If the jitter frequency is an odd multiple of half the line frequency (i.e., $f_j = mf_h / 2$, for $m = 1, 3, 5, \ldots$), E(t) remains constant, producing and undetectable offset in average brightness. If B is large enough, other jitter frequencies can cause a distracting interference pattern consisting of darkened or lightened horizontal bars. The width of the horizontal bars depends upon the frequency of the predominant jitter component.

An estimate of the maximum permissible jitter level Δt, can be obtained by way of (7) and the worst-case field-time waveform distortion specification of the RS-250B facilities standard [5]. For a maximum peak-to-peak deviation from flatness of 3 IRE units, Δt must be less than 13.4 nsec peak-to-peak. In practice, Δt must be much less than this in order to allow for other sources of field-time distortion. This level of jitter is also not likely in that it would result in unacceptable picture quality for broadcasting purposes [6].

B.Effect of Timing Jitter on the Multiple-Sample-per-Line Method

The equation that describes the dc clamping error for the case where N samples are averaged in each line is derived [see Appendix B] in a similar fashion as eq (8). Since the sampling interval is $1/f_S$ instead of $1/f_h$, the dc clamping error for any value of t becomes

*The IRE (Institute of Radio Engineers now IEEE) unit is defined as 1/100 of the signal level between blanking and peak white.

$$E(t) = -\frac{1}{N}\sum_{n=0}^{N-1}\left(A\sin\left\{2\pi f_{sc}\left[t-\frac{n}{f_s} + B\sin\left(2\pi\frac{nf_j}{f_s}+\phi_j\right)\right]+\phi_{sc}\right\}\right) \qquad (9)$$

where f_s is the non-jittered sampling rate.

Although this equation is difficult to analyze by inspection, computer analysis has shown that the resulting E(t) is approximately the same as that obtained under the same conditions with the one-sample-per line method. For example, if we use the same peak jitter deviation (B = 6.7ns), and arbitrarily set $\phi_j = 0°$, the maximum error of 1.636 IRE units occurs at $f_j = 4.2$MHz, when $\phi_{sc} = 46.6°$. This is shown in Fig. 8. Varying f_{sc} and f_j causes the shape of the curve to change in a cyclic manner, but at no time does the peak-to-peak error exceed 3.27 IRE units. Other than the fact that this method is more effective in averaging short-duration transients, there appears to be no distinct advantage of this method over the one-sample-per-line method, at least, in terms of the maximum error generated by a periodic jitter component.

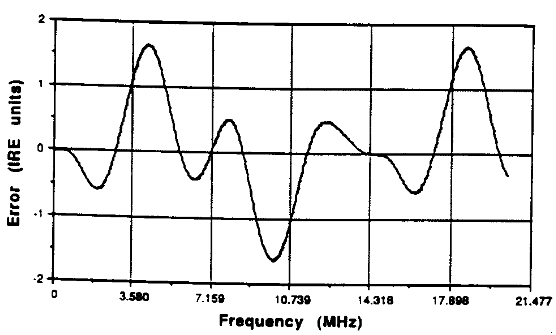

Fig. 8 Clamping error vs. Sampling jitter frequency for the multiple-samples-per-line averaging technique.With $f_s = 4f_{sc}$, $\phi_{sc} = 46.6°$, $B = 6.7$ns, $\phi_j = 0°$, maximum error of 1.636 IRE occurs for jitter frequency of 4.2mHz.

IV. IMPLEMENTATION AND EVALUATION

A. Circuit Description

The two hybrid clamping algorithms just described have been implemented in the form of a single circuit module. This circuit was fabricated on a high-density wire-wrap board and has been integrated into our digital video simulator [3] for evaluation. Emitter-coupled logic (ECL) technology is used for system compatibility and to allow operation at relatively high (28 Msamples/s) sampling rates. Hybrid sync-tip clamping and conventional analog clamping options are also available on the same circuit module.

The one-sample-per-line estimate is computed as shown in Fig. 9. In this configuration, a single sample from the color burst interval is averaged with the previous line's sample to obtain $\hat{D}(i,j)$. Depending upon how this estimate compares with the desired reference codeword, a binary counter is incremented or decremented by one count, or is maintained in the "hold" state. A 12-bit digital-to-analog (D/A) converter translates this long-term accumulation into a corresponding correction voltage for the analog clamper. This method of digital clipping and integration serves to dampen the response of the dc restorer and prevent instability.

With a slight modification, this same circuit synthesizes the second clamping algorithm. As shown in Fig. 10, the only difference is that N samples are averaged from each color burst interval. Synchronous control circuitry in the digitizer ensures that the correct samples are selected for each algorithm and that computations are inhibited during the vertical sync time. In all cases, the actual clamping takes place during a 1.2µs portion of the horizontal sync time. This prevents the analog clamper from interfering with back porch sampling and eliminates the possibility of a residual "glitch" within the color burst interval.

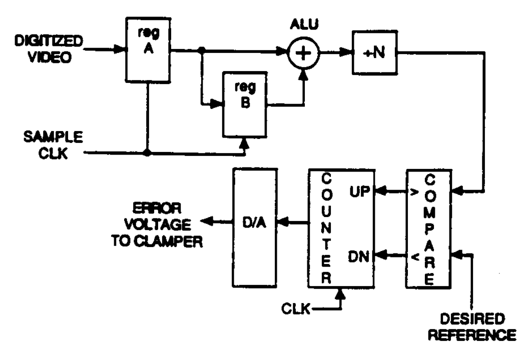

Fig. 9 Implementation of the one-sample-per-line algorithm.

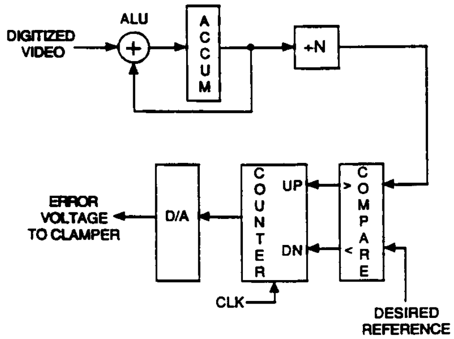

Fig. 10 Implementation of the multiple-samples-per-line algorithm.

B. Test Methods

The test set-up of Fig. 11 was used to evaluate the hybrid clamping algorithms in an actual system. A studio-quality color camera provided images and color-bar patterns for the test, while the output video was observed on a color monitor and oscilloscope. The one-sample-per-line and multiple-samples-per-line algorithms were programmed to stabilize the blanking level at digital code 010000000 (128 out of 512). The hybrid sync-tip clamper was programmed to stabilize the sync tip at digital code 000000001. The analog clamper that was used for comparison purposes was referenced to 0 VDC.

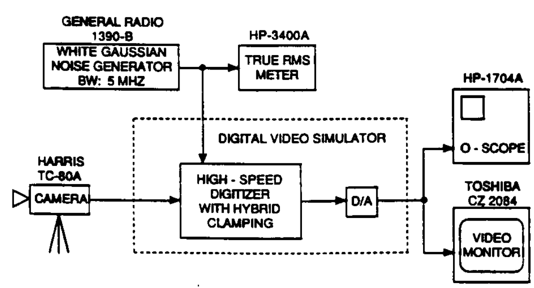

Fig. 11 Test set-up for measuring the noise and jitter thresholds of the hybrid clampers.

Proper operation of the clamping algorithms was first confirmed with a clock having very little jitter. This clock was synthesized directly from the camera's subcarrier reference so that the final sampling clock had periodic (3.58 MHz) jitter of less than 0.5 $ns_{p\text{-}p}$. To evaluate clamping performance in the presence of significant jitter, the clock synthesizer of the digitizer was phase-locked to a jittered f_h reference derived from the composite signal itself. For the noise vulnerability test, white Gaussian noise was added to the signal prior to low-pass filtering and clamping but after the reference extraction circuitry. The amplitude of the injected noise was steadily increased until disturbances could just be noticed on the color monitor.

C. Test Results

Under low clock jitter, high SNR conditions, all of the test clampers worked well with no detectable degradation. As the jitter level was increased, the performance of the hybrid sync-tip clamper and the conventional keyed clamper remained unaffected. This is to be expected since the signal slope is, essentially, zero during the sync time. The one-sample-per-line and multiple-samples-per-line hybrid clampers, on the other hand, each produced a slight flicker whenever the periodic plus random jitter reached 13 $ns_{p\text{-}p}$ or was sufficient to cause a 3.2 IRE variation in the output dc level. This observation is consistent with the jitter limits calculated in Section III.

When random amplitude noise was added to the signal, all three hybrid clampers performed well as long as the peak signal-to-rms noise ratio was greater than 42dB. At lower SNRs, a slight flicker could sometimes be observed. This flickering did not become much worse even as the SNR was lowered further, because of the digital clipping and integration incorporated in the hybrid clampers. These results were obtained consistently with sampling rates of $2f_{sc}$ (sub-Nyquist sampling), $\frac{8}{3}f_{sc}$, and $4f_{sc}$. Increasing the value of N (where appropriate) to a maximum of 8 samples, did not result in an appreciable increase in the SNR threshold.

In the case of the conventional keyed clamper, flickering did not occur until the peak signal-to-rms noise ratio was lowered to 35dB. This is primarily due to the fact that the clamping reference is a fixed voltage and independent of the signal. Conventional clamping methods therefore, might be more appropriate in low SNR applications (for example, in home television receivers). Averaging a greater number of samples would certainly improve the SNR threshold of the proposed hybrid clampers, although stable clock signals would still be necessary for reliable operation.

V. CONCLUSIONS

In this paper, we have examined two algorithms that are potentially useful in NTSC digital video equipment. Combinations and variations of these two algorithms can be used to compute the blanking level value from the digitized samples of the color-burst interval. When used in the feedback path of a hybrid clamper, drift errors are eliminated, SNR is improved due to better matching of the input signal to the A/D converter, and there are no residual transients as a result of clamping through the burst. Additionally, blanking or sync-tip levels are automatically stabilized at a predetermined digital output code.

Hybrid clampers that incorporate these algorithms, at least in their basic forms, are inherently sensitive to sampling clock jitter because of the steep signal slope of the 3.58 MHz subcarrier reference. These clampers have also been found to be more vulnerable to noise than a conventional keyed clamper since the clamping reference is derived from the signal itself. Averaging a greater number of samples (over an entire field for example) would improve this performance, but a stable sampling pulse would still be required for reliable operation. For this reason these clampers are best suited for A/D interfacing in a studio or closed circuit environment.

APPENDIX A
THE EFFECT OF SINUSOIDAL JITTER ON THE ONE-SAMPLE-PER-LINE ALGORITHM

Since one sample is to be taken at the same horizontal position in each line, the color burst should be sampled at intervals of $1/f_h$ as indicated in Fig. A.1(a). However, if the clock is jittered in a sinusoidal fashion, each sampling point will be advanced or retarded by an amount $\Delta t_n = B\sin\left(2\pi f_j t_n + \phi_j\right)$ as shown in Fig. A.1.(b). The calculated clamping error for line 2 is

$$E(t_2) = D(t_2 + \Delta t_2) - \frac{D(t_1 + \Delta t_1) + A\sin\left[2\pi f_{sc}(t_1 + \Delta t_1) + \phi_{sc}\right]}{2} - \frac{D(t_2 + \Delta t_2) + A\sin\left[2\pi f_{sc}(t_2 + \Delta t_2) + \phi_{sc}\right]}{2} \quad (A.1)$$

Assuming that the dc component of the signal has remained constant for the last two lines, $D(t_1 + \Delta t_1) = D(t_2 + \Delta t_2)$ so that

$$E(t_2) = -\left\{\frac{A\sin\left[2\pi f_{sc}(t_1 + \Delta t_1) + \phi_{sc}\right]}{2} + \frac{A\sin\left[2\pi f_{sc}(t_2 + \Delta t_2) + \phi_{sc}\right]}{2}\right\} \quad (A.2)$$

This expression can be generalized for any time t by letting $t_2 = t$ and by redefining f_j such that $\Delta t_2 = B\sin\phi_j$. The present subcarrier sample is now taken at time $\tau_2 = t + B\sin\phi_j$, while the previous (first) sample is taken at time

$$\tau_1 = t - \frac{1}{f_H} + B\sin\left(2\pi f_j \cdot \frac{1}{f_H} + \phi_j\right)$$

Substituting these values into (A.2), we obtain

$$E(t) = -\frac{A\sin\left\{2\pi f_{sc}\left[t - \frac{1}{f_H} + B\sin\left(2\pi\cdot\frac{f_j}{f_H} + \phi_j\right)\right] + \phi_{sc}\right\}}{2} - \frac{A\sin\left[2\pi f_{sc}\left(t + B\sin\phi_j\right) + \phi_{sc}\right]}{2} \quad (A.3)$$

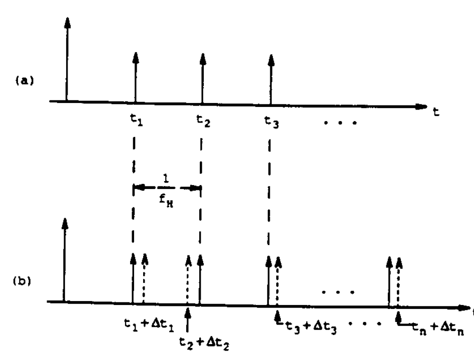

Fig. A.1 Sampling error caused by jitter: (a) normal uniform sampling, (b) nonuniform sampling due to jitter.

APPENDIX B

THE EFFECT OF SINUSOIDAL JITTER ON THE MULTIPLE-SAMPLES-PER-LINE ALGORITHM

The derivation of the clamping error equation for the case where multiple samples are taken from the center of a single color-burst interval is similar to the development of Appendix A, except that the sampling interval is $1/f_s$ rather than $1/f_h$.

If we, again redefine f_j such that the present sample is being taken at time $\tau_n = t + B\sin\phi_j$, the previous samples are taken at times

$$\tau_{n-1} = t - \frac{1}{f_s} + B\sin\left[2\pi f_j \cdot \frac{(1)}{f_s} + \phi_j\right]$$

$$\tau_{n-2} = t - \frac{2}{f_s} + B\sin\left[2\pi f_j \cdot \frac{(2)}{f_s} + \phi_j\right]$$

$$\tau_{n-3} = t - \frac{3}{f_s} + B\sin\left[2\pi f_j \cdot \frac{(3)}{f_s} + \phi_j\right] \quad \text{(B.1)}$$

$$\bullet$$
$$\bullet$$
$$\bullet$$

$$\tau_{n-N+1} = t - \frac{N-1}{f_s} + B\sin\left[2\pi f_j \cdot \frac{(N-1)}{f_s} + \phi_j\right].$$

Since the calculated clamping error is defined as

$$E(t) = D(t) - \hat{D}(t),$$

we obtain

$$E(t) = -\frac{1}{N}\sum_{n=0}^{N-1}\Bigg(A\sin\Bigg\{2\pi f_{sc}\Bigg[t - \frac{n}{f_s} + B\sin\left(2\pi \cdot \frac{nf_j}{f_s} + \phi_j\right)\Bigg] + \phi_{sc}\Bigg\}\Bigg) \quad \text{(B.2)}$$

This assumes that D has remained constant, so that E(t) reflects only the error caused by the sinusoidal jitter component.

REFERENCES

1. Y. Eto, et al, "Digital Processing Amplifier and Color Encoder," *SMPTE J.*, Vol. 87, pp. 15-19, Jan. 1978.

2. K.B. Benson, ed, *Television Engineering Handbook.* New York: McGraw-Hill, 1986.

3. N.R. Cox, "A High-Speed Programmable Digitizer for Real-Time Video Compression Experiments," Proceedings SPIE Visual Communications and Image Processing '91 Conf., Boston, MA, Nov. 10-13, 1991, vol. 1605, pp. 906-915.

4. S. Doba and J.W. Rieke, "Clampers in Video Transmission," *AIEE Transactions*, Vol. 69, pp. 477-487, 1950.

5. "Electrical Performance Standards for Television Relay Facilities," Electronic Industries Association (EIA), Doc. EIA RS-250-B, Sept. 1976.

6. V.G. Devereux, "Pulse Code Modulation of Video Signals: Subjective Tests on Acceptable Limits for Timing Jitter in the Decoded Analogue Samples," BBC Research Department Report No. 1971/42, 1971.